Proximal Probe Characterization of Nanoscale Charge Transport Properties in Co/SiO_2 Multilayer Structures

D.M. SCHAADT,[1] E.T. YU,[1,3] S. SANKAR,[2] and A.E. BERKOWITZ[2]

1.—University of California at San Diego, Department of Electrical and Computer Engineering, La Jolla, California 92093. 2.—University of California at San Diego, Center for Magnetic Recording Research, La Jolla, California 92093. 3.—e-mail: ety@ece.ucsd.edu

We have used scanning force microscopy to study localized charge injection and subsequent charge transport in discontinuous Co/SiO_2 multilayer structures. Charge was injected by applying a bias voltage pulse between a conductive proximal probe tip and the sample. Electrostatic force microscopy was used to image charged areas, to determine quantitatively the amount of stored charge, and to characterize charge transport. Charge was deposited controllably and reproducibly within areas ~20–50 nm in radius and an exponential decay in the peak charge was observed. The decay times were observed to be dependent on the nominal Co film thickness and on the sign of the deposited charge, with longer decay times for positive charge than for negative charge. These results are interpreted as a consequence of Coulomb-blockade effects, considering charge transport both within the Co layer as well as from the Co layer into the Si substrate.

Key words: Discontinuous metal/insulator multilayers, Coulomb-blockade, electrostatic force microscopy, scanning probe microscopy

INTRODUCTION

Discontinuous metal/insulator multilayers and related thin-film structures exhibit a variety of properties of importance for potential applications in high-density information storage and magnetic field sensing. These materials consist of metal nanoclusters embedded within an insulating matrix, and in specific cases, e.g. $[SiO_2/Co]_n$–SiO_2, have been shown to exhibit negative magnetoresistance due to spin-polarized tunneling between the metal particles, saturation of this magnetoresistance at low magnetic fields[1,2] and storage of electrical charge in the nanoclusters.[3] A novel highly-sensitive magnetic field sensor based on the combination of these charge storage effects with tunnel-magnetoresistance has recently been proposed and demonstrated.[4] The design and optimization of devices incorporating these materials require a detailed understanding of the relevant electrical transport properties, which are usually investigated in a global manner due to the large electrode area typically employed. However, scanning probe techniques make possible the characterization and manipulation of these properties on a highly localized basis.

(Received November 22, 1999; accepted June 14, 2000)

In this paper, we describe detailed characterization and analysis of proximal-probe-induced local charge deposition into and removal from Co nanoclusters embedded in an insulating SiO_2 film deposited on a Si substrate. Electrostatic force microscopy (EFM) was used to image charged areas, to determine quantitatively the amount of stored charge, and to characterize charge transport within the Co layer and into the Si substrate. Controlled deposition of small numbers of electrons by a proximal probe is demonstrated and quantified. Measurements of decay times for positive and negative charge as a function of nominal Co layer thickness are presented, and the dynamics of the charge decay for positively and negatively charged nanoclusters is analyzed as a consequence of Coulomb-blockade effects at room temperature, considering a detailed model for charge transport within the Co layer as well as from charge Co nanoclusters into the Si substrate.

SAMPLE PREPARATION AND STRUCTURE

Samples for the charging experiments were prepared by alternating sputtering from two about

~2.5 nm in thickness. The Co was dc sputtered and the SiO_2 was rf sputtered. Deposition was performed at room temperature with 2 mtorr Ar pressure; the base pressure in the sputtering system was ~10^{-7} torr. The nominal deposited film structures were SiO_2(3 nm)/Co(1.0–2.0 nm)/SiO_2(3 nm) as determined from the deposition times and rates (0.9–1.3 nm/min for the Co and 2.0–3.0 nm/min for the SiO_2), which were calibrated by low-angle x-ray reflection. Transmission electron microscopy (TEM) studies have shown that, when deposited on SiO_2, the Co layer is discontinuous, as depicted schematically in Fig. 1.[5,6] The nanoscale structure of the Co layer depends sensitively on the nominal Co film thickness, and consists of isolated spherical Co nanoclusters for films with a nominal thickness of approximately less than 1.4 nm and of a chain-like arrangement of spherical Co nanoclusters for nominal thicker films.

EXPERIMENTAL PROCEDURE

Scanning probe studies were performed at room temperature under ambient conditions using a Digital Instruments MultiMode™ Scanning Probe Microscope[7] with a heavily doped p-type Si tip. Sample charging was performed during TappingMode™ operation by holding the tip at the center of the scan area for 10 sec with a bias voltage applied to the tip and the sample grounded, as shown in Fig. 1. During the charging process, current flows from the tip into the Co layer as well as from the Co layer into the substrate in a manner analogous to the charging process in a floating-gate MOS structure. These currents are initially different due to the different oxide thicknesses and equilibrate over time as a consequence of the adjustments in the electric fields across the oxide layers due to the charge build-up in the Co cluster.[8] Once equilibrium is reached, the charge in the Co cluster does not increase any further and its value is determined by the tip-sample capacitance. We observed little variation in sample charging for charging times longer than 5 sec.

EFM was used to image charged regions and to estimate the total stored charge. A series of EFM images obtained before and after charging at different bias voltages is shown in Fig. 2. Charged areas are observed as peaks or dips in the EFM images, depending on the relative sign of the charging and imaging voltages. No charging was observed in a control sample in which no Co layer was present. Due to the difference in retention times, application of a voltage pulse of opposite sign (± 10 V for 10 sec) to the charged area about 30 sec after charging erases the positive charge almost completely, while the negative charge is overwritten by positive charge, as shown in Fig. 2c.

The contrast observed in the EFM image may be used to calculate the total stored charge.[3] Specifically, the shift Δf in the resonant frequency of the cantilever is related to the force gradient $F' \equiv dF/dz$ by the expression $\Delta f = -f_0(z_0)/(2k)$, where z_0 = 20 nm is the lift height during EFM imaging, f_0 = 232 kHz the cantilever resonant frequency, and k the cantilever spring

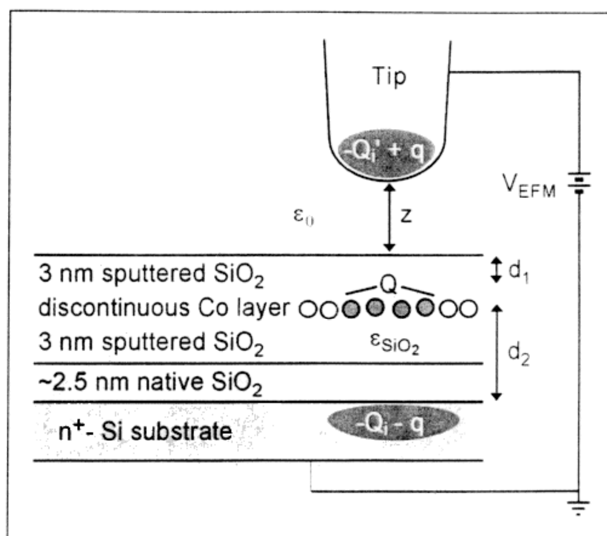

Fig. 1. Schematic diagram showing the SiO_2/Co/SiO_2/Si sample structure and the sample and tip geometry in the scanning probe microscope. The charge Q deposited in the Co nanocluster layer induces image charges –Qi in the Si substrate and –Qi′ in the tip. Additional charges q and –q are present due to the voltage VEFM applied during imaging.

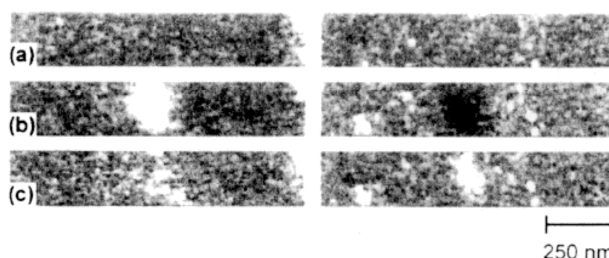

Fig. 2. EFM images obtained with imaging voltage VEFM = 1 V (a) before charging, (b) after charging with +12 V (left) and –12 V (right) for 10 sec, and (c) after erasing with bias voltages of –10 V (left) and +10 V (right) for 10 sec, respectively. Charged areas are observed as bright and dark spots.

constant, which was estimated from the cantilever geometry to be 90 ± 10 N/m. The force F(z) arises from Coulomb interactions among the stored charge, its image charges in the tip and Si substrate, and the induced charges due to the voltage V_{EFM} applied during imaging. From an electrostatic analysis of the tip-sample system modeled using a simple parallel-plate geometry, the force gradient, which contributes to contrast differences between charged and uncharged areas, is found to be given approximately by[3]

$$F'(z) \approx -\frac{2d_2 Q V_{EFM}}{\varepsilon_{SiO_2}(z + (d_1 + d_2)/\varepsilon_{SiO_2})^3} \qquad (1)$$

where d_1 and d_2 are the thicknesses of the top and bottom oxide layer, respectively, ε_{SiO_2} the relative dielectric constant of SiO_2, and z the tip-sample distance. Thus, the final contrast observed is proportional to the stored charge Q and to V_{EFM}. Using the values for f_0, k, z, d_1, and d_2 given above, the total charge Q is then given by $Q \approx 18$ e/V·Hz $V_{EFM}\,\Delta f$.

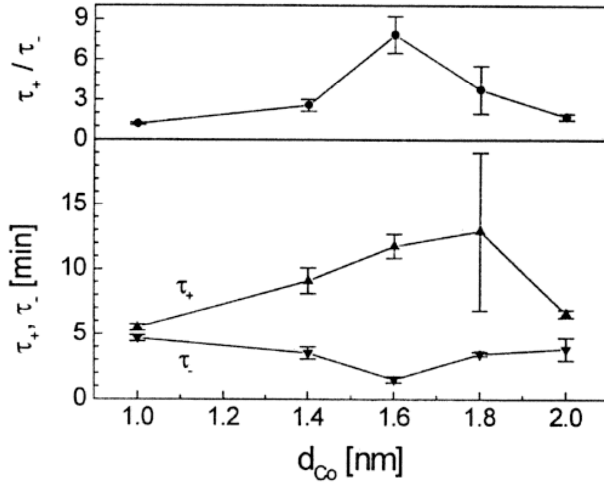

Fig. 3. Retention times τ_+ for positive charge and τ_- for negative charge and the ratio τ_+/τ_-, plotted as functions of nominal Co film thickness, as determined from exponential fits to the peak-height decrease in the EFM images after charging with +12 V and −12 V for 10 sec, respectively. Because a fixed time window was used to determine the retention times, the exponential fit to the slow decay in positive charge for d_{Co} = 1.8 nm resulted in a large error bar.

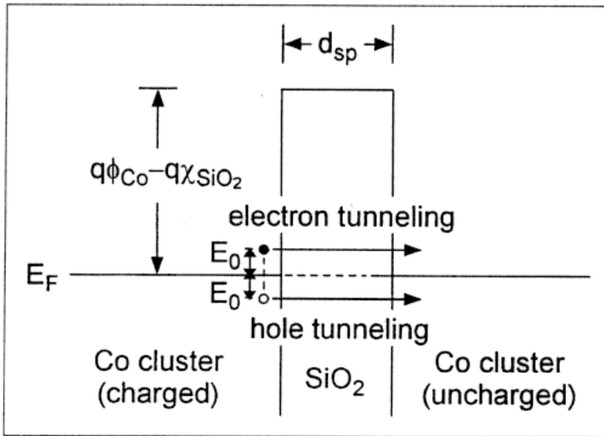

Fig. 4. Band diagram for charge transport within the Co film, where E_0 is the Coulomb-blockade energy, dsp the spacing between Co clusters, ϕ_{Co} the Co workfunction, χ_{SiO_2} the SiO_2 electron affinity, and q the electron charge. Holes and electrons experience different barrier heights in the tunneling process due to the Coulomb-blockade energy.

RESULTS AND DISCUSSION

We have previously shown, for a sample with a Co film nominally 1.4 nm in thickness, that charging at ±12 V deposits or removes approximately one electron per one to two Co nanoclusters; in addition we observed exponential charge decay with the retention time τ_+ for positive charge being significantly larger than the retention time τ_- for negative charge.[3] Discharging was assumed to occur primarily via tunneling from the charged Co clusters into the Si substrate. The difference in retention times for positive and negative charge was interpreted as a consequence of the difference in barrier heights for escape of positive and negative charge, given, respectively, by $\phi_+ = \phi_0 + E_0$ and $\phi_- = \phi_0 - E_0$, where $\phi_0 = \left(\phi_{Co} + \chi_{Si} - 2\chi_{SiO_2}\right)/2$ is the barrier height of the Co − SiO_2 − Si tunnel barrier, ϕ_{Co} the Co workfunction, χ_{Si} the Si electron affinity, χ_{SiO_2} the SiO_2 electron affinity, and q the electron charge. This difference arises from the non-negligible Coulomb-blockade energy $E_0 = q^2/(2C_{Co})$ of a single Co cluster with capacitance C_{Co}. Since the dependence of the tunneling probability T on barrier height ϕ and barrier thickness d is given approximately by $T \propto \exp\left(-2d\sqrt{2mq\phi}/\hbar\right)$ and the retention time is inversely proportional to T, the relation between the decay times should be given approximately by

$$\frac{\tau_+}{\tau_-} \approx e^{\frac{2\sqrt{2m}}{\hbar} d_{SiO_2}\left(\sqrt{q\phi_0 + E_0} - \sqrt{q\phi_0 - E_0}\right)}$$

$$\approx 1 + \frac{2\sqrt{2m}}{\hbar}\frac{d_{SiO_2}}{\hbar}E_0$$

$$\text{for } E_0 << q\phi_0, \qquad (2)$$

where m is the electron mass and d_{SiO_2} the thickness of the lower SiO_2 layer. The Coulomb-blockade energy E_0 depends strongly on the size and shape of the Co cluster, and it was therefore expected that the retention times would depend strongly on the nanoscale structure of the Co layer. Specifically, this simplified model suggests that the difference in retention times should be large for small nominal Co film thickness d_{Co}, where the Coulomb-energy E_0 is large, and should decrease with increasing d_{Co} as E_0 decreases.

To test the above model, we measured the charge retention times τ_+ and τ_-, as well as their ratio τ_+/τ_-, as functions of nominal Co film thickness d_{Co}. The retention times were determined from exponential fits to the peak-height decrease over time after charging with a ±12V bias voltage pulse 10 sec in duration. The results of these measurements are shown in Fig. 3. τ_+ first increases with increasing d_{Co}, reaching a maximum for $d_{Co} \approx$ 1.6–1.8 nm, and then decreases and approaches τ_-. In contrast, the negative charge retention time τ_- shows the opposite behavior, first decreasing with increasing d_{Co}, reaching a minimum for d_{Co} = 1.4 nm, and then increasing with increasing d_{Co}. As expected, the retention time for positive charge is larger than that for negative charge over the entire range of values of d_{Co}, and the difference in retention times becomes smaller as d_{Co} increases. However, the simplified model described above does not predict the observed retention time behavior for nominal Co film thicknesses d_{Co} < 1.6–1.8 nm.

To explain more completely the dependence of the retention times on d_{Co}, we must consider that discharging can occur within the Co layer as well as from the Co particles into the Si substrate. The total retention times τ_+ and τ_- will then be given by

$$\frac{1}{\tau_{+,-}} = \frac{1}{\tau_{+,-}^{in}} + \frac{1}{\tau_{+,-}^{out}} \qquad (3)$$

where τ_+^{in} and τ_-^{in} are the characteristic retention times for charge transport within the Co layer and τ_+^{out}

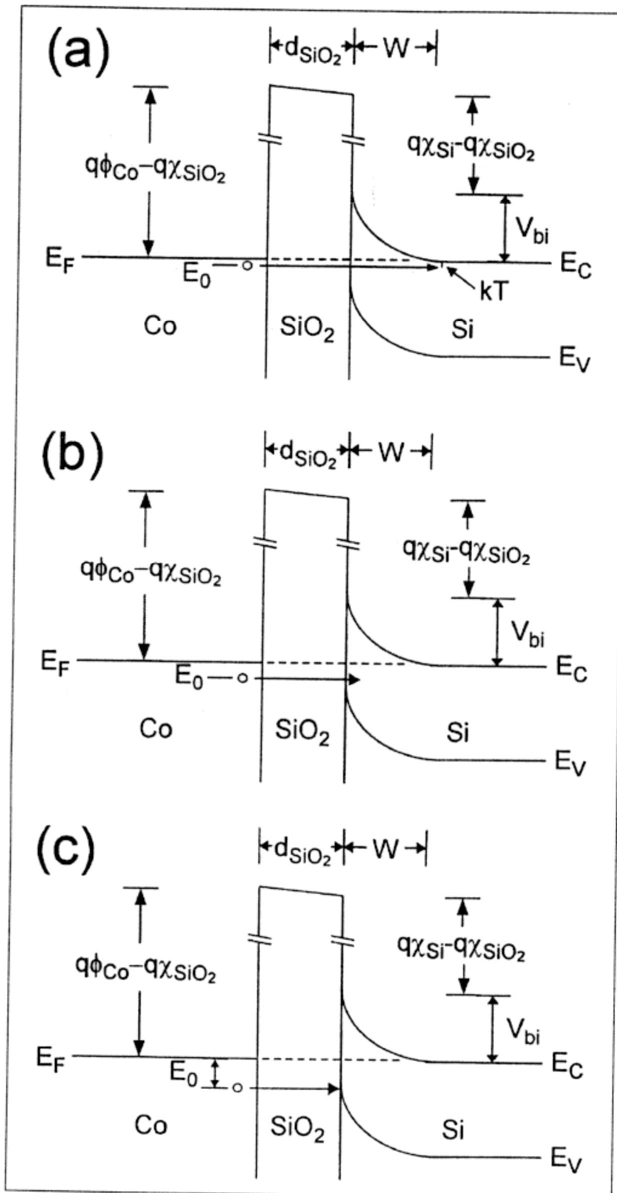

Fig. 5. Band diagrams for escape of positive charge from a Co cluster into the Si substrate, where W is the depletion width, V_{bi} the build-in potential, E_C the conduction band level, and E_V the valence band level. (a) For small Coulomb-blockade energies, inelastic tunneling of a hole from the Co cluster into the conduction band of the semiconductor is possible. (b) For moderate Coulomb-blockade energies, no hole states exist in the Si layer at energies near the hole energy, making tunneling much less probable. (c) For large Coulomb-blockade energies, tunneling of holes into the valence band of the semiconductor becomes possible.

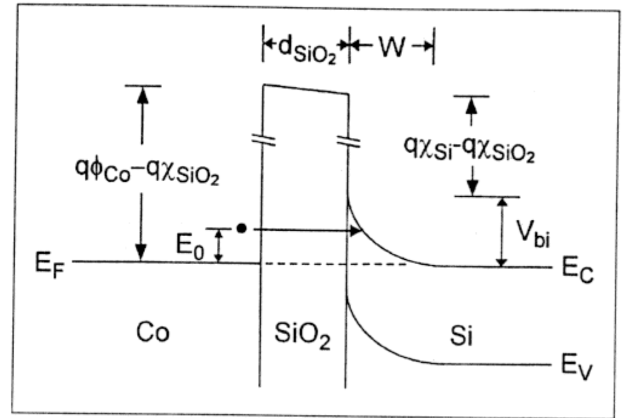

Fig. 6. Band diagram for escape of negative charge from a Co cluster into the Si substrate. Due to the band bending in the semiconductor, the tunnel barrier width depends on the Coulomb-blockade energy.

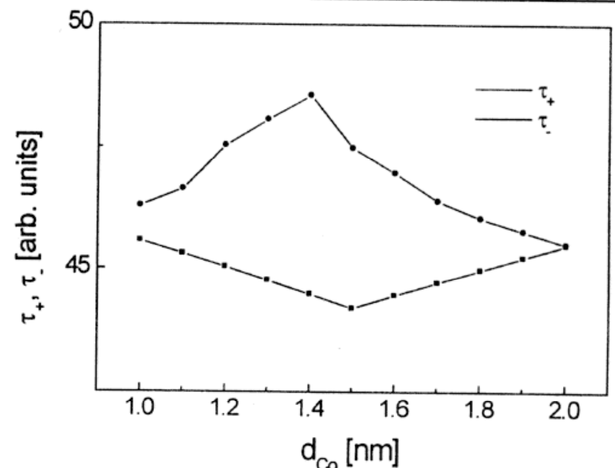

Fig. 7. Computed values of τ_+ and τ_- as functions of nominal Co film thickness, obtained using Eqs. 3–7. The computed results are in qualitative agreement with the discharging behavior shown in Fig. 3. Due to the uncertainties in the Coulomb-blockade energy, the spatial dimensions and experimental measurements, the experimentally measured retention times are not quantitatively reproduced.

and τ_-^{out} pertain to charge transport from the Co layer into the Si substrate. Since the retention times depend strongly on the barrier width as well as the Coulomb-blockade energy, it is necessary to account for the nanoscale structure of the Co layer. It is known from TEM micrographs that the Co layer consists of isolated spherical clusters for a nominal layer thickness of about 1.4 nm and below, and of chain-like arrangements of connected spherical particles for nominally thicker films.[5,6] Since the Co clusters increase in size with increasing nominal thickness above 1.4 nm, the capacitance of these clusters increases and thus the Coulomb-blockade energy decreases. As the nominal film thickness decreases below about 1.4 nm, the Co particles remain spherical and the spacing between the particles increases. Thus, the Coulomb-blockade energy remains fairly constant below nominal thicknesses of about 1.4 nm.

The band diagram for discharging within the Co layer is shown in Fig. 4. For discharging within the Co layer, the retention times are given by

$$\tau_{+,-}^{in} \propto e^{\frac{2\sqrt{2m_{SiO_2}^{h,e}}}{\hbar} d_{sp} \sqrt{q\phi_{Co} - q\chi_{SiO_2} \pm E_0}} \qquad (4)$$

where d_{sp} is the spacing between the Co clusters and $m_{SiO_2}^{h}$ and $m_{SiO_2}^{e}$ are the effective masses of holes and electrons in SiO_2, respectively. τ_+^{in} and τ_-^{in} increase exponentially with increasing d_{sp} as the nominal Co film thickness decreases below 1.4 nm, and approach

Equation 5

$$\tau_+^{out} \propto e^{\frac{2\sqrt{2q}}{\hbar}\int_0^{d_{SiO_2}+W} \sqrt{m^h\phi(x)}dx} \approx e^{\frac{2\sqrt{2}}{\hbar}\left(d_{SiO_2}\sqrt{m^h_{SiO_2}(q\phi_0+E_0)}+\frac{\pi}{2}W\sqrt{qm^h_{Si}V_{bi}}\left(1+\frac{E_0}{qV_{bi}}\right)-W\sqrt{2m^h_{Si}E_0}\right)}$$

each other as E_0 decreases for Co films with nominal thickness above 1.4 nm.

Band diagrams for discharging from a positively charged Co cluster into the Si substrate are shown in Fig. 5. We must consider three cases. For small Coulomb-blockade energies $E_0 \leq kT$, where k is the Boltzmann constant, a hole will tunnel from the Co cluster into the conduction band of the Si substrate as shown in Fig. 5a, and τ_+^{out} is given in Eq. 5. Equation 5 shows that the barrier height is given by $\phi(x) = \phi_{Co} - \chi_{SiO_2} + E_0 / q + (\chi_{Si} - \phi_{Co})x / d_{SiO_2}$ for $0 \leq x \leq d_{SiO_2}$ and $\phi(x) = V_{bi} + E_0 / q - V_{bi}(x - d_{SiO_2})^2 / W^2$ for $d_{SiO_2} < x < d_{SiO_2} + W$, m_{Si}^h is the effective hole mass in Si, $W = \sqrt{2\varepsilon_{Si}V_{bi} / (qN_D)}$ is the depletion width, εSi is the Si permittivity, N_D the dopant concentration in the Si, and V_{bi} the built-in potential. As the Coulomb-blockade energy increases with decreasing d_{Co}, τ_+^{out} increases.

For Coulomb-blockade energies in the range $kT < E_0 < E_g - qV_{bi} - kT$, where E_g is the Si bandgap, no hole states exist on the semiconductor side, as shown in Fig. 5b. The tunneling probability becomes very small and thus the retention time τ_+^{out} reaches a maximum value. According to Eq. 3, the total retention time τ_+ for positive charge will be limited by τ_+^{in} in this regime.

Finally, for Coulomb energies $E_0 \geq E_g - qV_{bi} - kT$, tunneling of holes into the valence band is possible, as shown in Fig. 5c, and τ_+^{out} is given by

$$\tau_+^{out} \propto e^{\frac{2\sqrt{2m^h_{SiO_2}}}{\hbar}d_{SiO_2}\sqrt{q\phi_0+E_0+(E_g-qV_{bi})/2}} \quad (6)$$

The band diagram for tunneling from a negatively charged Co cluster into the Si substrate is shown in Fig. 6. The tunneling barrier width depends on the Coulomb-blockade energy E_0 due to the band bending within the Si substrate layer. τ_-^{out} is then given, in a manner analogous to that used to obtain Eq. 5, by

$$\tau_-^{out} \propto e^{\frac{2\sqrt{2}}{\hbar}\left(d_{SiO_2}\sqrt{m^e_{SiO_2}(q\phi_0-E_0)}+\frac{\pi}{2}W\sqrt{qm^e_{Si}V_{bi}}\left(1-\frac{E_0}{qVi_{bi}}\right)\right)} \quad (7)$$

where m_{Si}^e is the effective electron mass in Si.

The expressions for $\tau_{+,-}^{in}$, $\tau_{+,-}^{out}$, and τ+,- derived in Eqs. 3–7 may be used to analyze the dependence of $\tau_{+,-}$ on d_{Co}. Since exact values for the Coulomb-blockade energies and the spacings between Co clusters are unknown, we assumed the following values, which were believed to be physically reasonable. A value of 3.1 nm was assumed for d_{sp} for d_{Co} = 1.0 nm, decreasing linearly to 3 nm for d_{Co} = 1.4 nm and then remaining constant for d_{Co} > 1.4 nm. E_0 was assumed to decrease linearly from 0.11 eV to 0.01 eV for d_{Co} increasing from 1.0 nm to 2.0 nm. The computed dependence of τ_+ and τ_- on d_{Co} qualitatively reproduces the experimentally observed dependence quite closely. However, discrepancies exist in the exact values due to the large uncertainties in both the above estimated values as well as in the measurements.

CONCLUSIONS

Scanning probe techniques were used to demonstrate and characterize local charge deposition and transport in Co nanoclusters embedded in an insulating SiO_2 matrix. Positive and negative charges can be deposited controllably and reproducibly. The charge decays over several minutes with part of it spreading out in the discontinuous Co film and the rest tunneling into the Si substrate. The charge retention times τ_+ for positive charge and τ_- for negative charge as well as their ratio depend strongly on the nanoscale structure of the discontinuous metal cluster film. These results were interpreted as a consequence of Coulomb-blockade effects, and a detailed model considering charge transport within the Co layer as well as from the Co cluster into the Si substrate was used to explain qualitatively the dependence of the retention times on the nanoscale Co film structure.

ACKNOWLEDGEMENTS

Part of this work was supported by ONR (Grant No. N00014-95-1-0996) and NSF (Award Nos. ECS95-01469 and DMR 9400439). ETY would like to acknowledge financial support from the Alfred P. Sloan Foundation.

REFERENCES

1. S. Sankar, B. Dieny, and A. E. Berkowitz, *J. Appl. Phys.* 81, 5512 (1997).
2. K.R. Coffey, T.L. Hylton, M.A. Parker, and J.K. Howard, *Scr. Metall. Mater.* 33, 1593 (1995).
3. D.M. Schaadt, E.T. Yu, S. Sankar, and A.E. Berkowitz, *Appl. Phys. Lett.* 74, 472 (1999).
4. D.M. Schaadt, E.T. Yu, S. Sankar, and A.E. Berkowitz, *Appl. Phys. Lett.* 75, 731 (1999).
5. S. Sankar, D.J. Smith, and A.E. Berkowitz, *Appl. Phys. Lett.* 73, 535 (1998).
6. B. Dieny, S. Sankar, M.R. McCartney, D.J. Smith, and A.E. Berkowitz, *J. Magn. Magn. Mater.* 185, 283 (1998).
7. MultiMode and TappingMode are trademarks of Digital Instruments, Santa Barbara, CA.
8. S.M. Sze, *Physics of Semiconductor Devices* (New York: John Wiley & Sons, 1981), p. 497.